

Towards Theranostics of Rheumatoid Arthritis: $^1\text{H}/^{19}\text{F}$ Imaging of Non-Steroidal Anti-Inflammatory Drugs in Hand and Wrist at 7 Tesla

Helmar Waiczies^{1,2}, André Kühne^{3,4}, Lukas Winter², Tobias Frauenrath², Werner Hoffmann³, Bernd Ittermann³, Sonia Waiczies^{1,2}, and Thoralf Niendorf^{2,5}
¹Magnetic Resonance Imaging in Immunology, Experimental and Clinical Research Center (ECRC), a cooperation of the Charité Medical Faculty and the Max Delbrück Center for Molecular Medicine, Berlin, Germany, ²Berlin Ultrahigh Field Facility (B.U.F.F.), Max Delbrück Center for Molecular Medicine, Berlin, Germany, ³Department of Medical Physics and Metrological Information, Physikalisches Technische Bundesanstalt, Berlin, Germany, ⁴Center for Medical Physics and Biomedical Engineering, Medical University of Vienna, Vienna, Austria, ⁵Experimental and Clinical Research Center (ECRC), Charité University Medicine Campus Berlin-Buch, Berlin, Germany

Introduction: Rheumatoid arthritis (RA) is a chronic and systemic inflammatory condition of the skeletal system that also affects adults within the prime of their work productivity. By targeting synovial tissue, cartilage and bone, RA is a debilitating condition since it significantly hinders the physical functioning and working capacity of an individual [1]. While the therapeutic armamentarium for RA is extensive, a comprehensive diagnosis of the disease (particularly knowledge of the exact location of inflammation) during early stages of disease is central for preventing and delaying further disease progression. New emerging MRI technologies to study cartilage composition include gadolinium enhanced cartilage imaging, ^{23}Na -MRI and T_2 relaxation mapping [2]. ^{19}F -MRI has become increasingly important for small animal imaging in multiple fields of pre-clinical research including cell tracking and detection of inflammation [3]. Since ^{19}F containing molecules are scarce in the human body, administration of exogenous fluorine containing compounds such as non-steroidal anti-inflammatory drugs (NSAIDs) will give a background free signal in ^{19}F MRI. This study involves the development of a double-tuned $^1\text{H}/^{19}\text{F}$ birdcage resonator and examines its applicability for hand and wrist ^{19}F imaging at 7 T following topical application of the NSAID 2-[[3-(Trifluoromethyl) phenyl]amino]benzoic acid.

Methods: Electromagnetic field (EMF) simulations with CST MWS (CST AG, Darmstadt, Germany) (Fig. 1A) were performed using the right arm of the voxel model "Billie" of the Virtual Family [4]. Simulations were conducted to assess SAR (Fig 1C) and B_1^+ (Fig. 1D) distribution. The coil was built using a design derived from initial simulations. Extended simulations were then performed for the final coil geometry. The 8-leg high-pass birdcage has a diameter of 10 cm and a length of 16 cm, one port was tuned to 279 MHz for ^{19}F and the other one to 297 MHz for ^1H (Fig 1B). Phantom and *in vivo* measurements were performed on a 7 T Siemens Magnetom using a 3D gradient-echo sequence modified for ^{19}F application. (GRE 3D TR/TE=15/1.0ms, Matrix 48x48, FOV 100x100, Slab 80mm, 16 slices 5mm, 64 averages, TA 12:20min). Proton images were acquired using a T_1 weighted turbo spin-echo sequence (TSE TR/TE=400/9ms, Matrix 384x384, FOV 100x100, 16 slices 5mm, TA 1min).

Results: SAR calculations from the EMF Simulation show that the maximum 10g local SAR of 16.2W/kg (@4W stimulated power) lies well within IEC 60601-2-33 limits (Fig 1C). Simulated B_1^+ gives a maximum of 114 $\mu\text{T}/\sqrt{\text{kW}}$ in the center of the voxel model (Fig 1D) and 116 $\mu\text{T}/\sqrt{\text{kW}}$ in a phantom with a relative permittivity of $\epsilon = 78$ and conductivity of $\sigma = 0.3\text{S/m}$ (Fig 1E). The measured B_1^+ on the proton channel is 97 $\mu\text{T}/\sqrt{\text{kW}}$ in the center of a cylindrical phantom with similar properties as used in the EMF-Simulation (Fig 1F). Figure 2 shows first *in vivo* images acquired with the present dual-tunable $^{19}\text{F}/^1\text{H}$ -birdcage at 7 T. Twenty minutes prior to imaging, the wrist of the volunteer received a 10g topical application of a cream containing the active compound 2-[[3-(Trifluoromethyl) phenyl]amino]benzoic acid at a concentration of 1mmol/l. Fig 2A shows the original ^{19}F GRE image and Fig 2B the masked and threshold filtered image of the same slice. Fig 2C shows the overlay of a T_1 W TSE proton image with the filtered ^{19}F image (red). The dotted line in the reference image (Fig 2D) depicts the position of the transversal slice in Fig 2A-C.

Discussion and Conclusions: The preliminary *in vivo* images acquired by the double-tuned $^1\text{H}/^{19}\text{F}$ birdcage resonator demonstrate the feasibility of hand- and wrist-imaging at 7 T. While the diagnostic quality of the acquired proton images still needs to be assessed in patients with inflammatory rheumatoid disease of the hands and wrist, first ^{19}F images of fluorine-containing NSAIDs such as 2-[[3-(Trifluoromethyl) phenyl]amino]benzoic acid are encouraging, and point towards the prospect of applying ^{19}F -MRI and NSAID therapy to the field of theranostics, for visualizing and measuring the concentration of the therapeutically-active compound reaching the inflammatory site in RA patients.

- Burton W, Morrison A, Maclean R, Ruderman E (2006) Systematic review of studies of productivity loss due to rheumatoid arthritis. *Occup Med (Lond)* 56: 18-27.
- Borrero CG, Mountz JM, Mountz JD (2011) Emerging MRI methods in rheumatoid arthritis. *Nat Rev Rheumatol* 7: 85-95.
- Ruiz-Cabello J, Barnett BP, Bottomley PA, Bulte JW (2011) Fluorine (^{19}F) MRS and MRI in biomedicine. *NMR Biomed* 24: 114-129.
- Christ A et al. (2010) The Virtual Family – development of surface-based anatomical models of two adults and two children for dosimetric simulations. *Phys Med Biol*. 2010, 55: N23-38

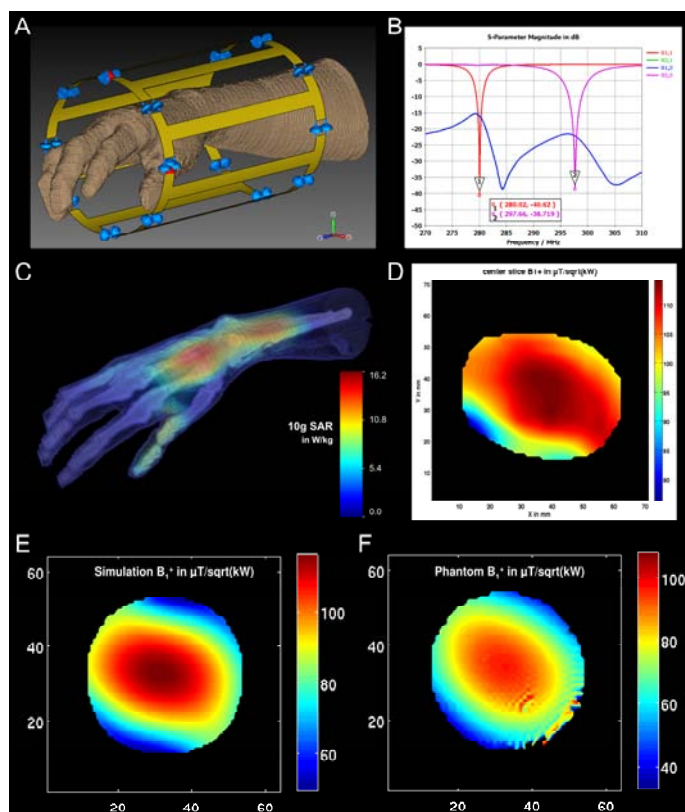


Figure 1: A) model of the $^{19}\text{F}/^1\text{H}$ birdcage with the right arm of the voxel model "Billie"; B) simulated S-Parameters of both ^{19}F and ^1H -channel; C) 3D MIP projection of the 10g SAR on the voxel model's arm; D) simulated B_1^+ field in the center of the coil using the voxel model; E) simulated and F) measured B_1^+ distribution in the center of the coil in a homogeneous phantom.

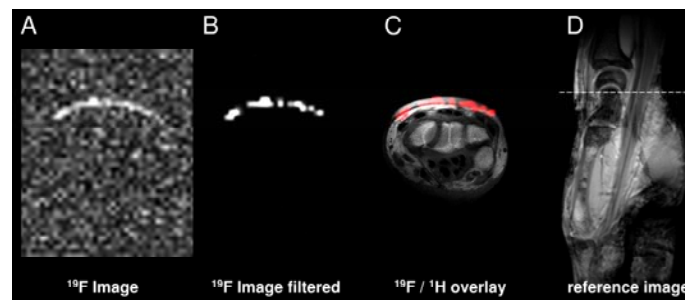


Figure 2: A) original ^{19}F GRE image; B) masked and threshold filtered ^{19}F GRE image; C) overlay of the ^{19}F GRE image (red) with the corresponding transversal slice of the wrist; D) sagittal reference image, dotted line depicts the position of the transversal slice.